Journal of Computational Mathematics
Vol.29, No.6, 2011, 639–660.

http://www.global-sci.org/jcm
doi:10.4208/jcm.1109-m11si03

MULTIPLE TEMPERATURE GAS DYNAMIC EQUATIONS FOR NON-EQUILIBRIUM FLOWS*

Kun Xu
Mathematics Department, Hong Kong University of Science and Technology, Hong Kong, China
Email: makxu@ust.hk
Zhaoli Guo
National Laboratory of Coal Combustion, Huazhong University of Science and Technology, Wuhan 430074, China
Email: zlguo@mail.hust.edu.cn

Abstract

In an early approach, a kinetic model with multiple translational temperature [K. Xu, H. Liu and J. Jiang, Phys. Fluids **19**, 016101 (2007)] to simulate non-equilibrium flows was proposed. In this paper, instead of using three temperatures in the x, y and z-directions, we define the translational temperature as a second-order symmetric tensor. Under the new framework, the differences between the temperature tensor and the pressure tensor will be explicitly pointed out. Based on a multiple stage BGK-type collision model and the Chapman-Enskog expansion, the corresponding macroscopic gas dynamics equations in three-dimensional space will be derived. The zeroth-order expansion gives 10 moment closure equations similar to that of Levermore [C.D. Levermore, J. Stat. Phys **83**, pp.1021 (1996)]. The derived gas dynamic equations can be considered as a regularization of the 10 moments equations in the first-order expansion. The new gas dynamic equations have the same structure as the Navier-Stokes equations, but the stress-strain relationship in the Navier-Stokes equations is replaced by an algebraic equation with temperature differences. At the same time, the heat flux, which is absent in Levermore's 10 moment closure, is recovered. As a result, both the viscous and the heat conduction terms are unified under a single anisotropic temperature concept. In the continuum flow regime, the new gas dynamic equations automatically recover the standard Navier-Stokes equations. Our gas dynamic equations are natural extensions of the Navier-Stokes equations to the near continuum flow regime and can be used for microflow computations. Two examples, the force-driven Poiseuille flow and the Couette flow in the transition flow regime, are used to validate the model. Both analytical and numerical results are presented. Theoretically, the Boltzmann equation can be also applied to the current multiple stage gas evolution model to derive generalized macroscopic governing equations in the near continuum flow regime. Instead of using Maxwellian as an expansion point in the Chapman-Enskog method, the multiple temperature Gaussian can be used as an expansion point as well.

Mathematics subject classification: 65C20, 76P05.
Key words: Gas-kinetic Model, Multiple Translational Temperatures, Generalized Gas Dynamics Equations.

1. Introduction

The transport phenomena, i.e., mass, heat, and momentum transfer, in different flow regimes are of a great scientific and practical interest. The classification of various flow regimes is based

* Received January 1, 2011 / Revised version received April 21, 2011 / Accepted April 21, 2011 / Published online November 15, 2011 /

on the dimensionless parameter, i.e., the Knudsen number, which is a measure of the degree of rarefaction of the medium. The Knudsen number, Kn, is defined as the ratio of the mean free path to a characteristic length scale of the system. In the continuum flow regime where $Kn < 0.001$, the Navier-Stokes equations with linear relations between stress and strain and the Fourier's law for heat conduction are adequate to model fluid behavior. For flows in the continuum-transition regime ($0.1 < Kn < 1$), the Navier-Stokes (NS) equations are known to be inadequate. This regime is important in many practical engineering problems. Hence, accurate models that give reliable solutions at low computational costs, would be useful.

One of the alternative approaches to simulating non-equilibrium flow is that based on moment closures. Grad's 13 moment equations are among the most important. They provide the time evolution of non-equilibrium quantities, such as stress and heat flux [3]. However, due to its hyperbolic nature, these equations lead to a well-known sub-shock problem inside a shock layer when the Mach number is larger than a critical value. To improve the validity of the 13 moment equations, based on the Chapman-Enskog expansion, Struchtrup and Torrilhon introduced terms of the super-Burnett order to the balance of pressure deviator and the heat flux vector in the moment equations and established regularized 13 moment (R13) equations that have much better performance in the non-equilibrium flow regime [4]. Another well-known moment system is Levermore's 10 moment closure, which follows his hierarchy of non-perturbative moment closures with many desirable mathematical properties [2]. These equations do not suffer from closure-breakdown deficiencies, and they always give physically realizable solutions due to non-negative gas distribution functions. However, the 10 moment Gaussian closure has no heat flux even though the Navier-Stokes viscous terms can be recovered in the continuum flow regime. In an effort to extend the Gaussian closure to include higher-order effects, Groth et al. formulated perturbative variants of the original moment closure with a new extended fluid dynamics model [5]. The most studied of these closures is a 35-moment closure. Recently, McDonald and Groth took a Chapman-Enskog-type expansion of either the moment equations or the kinetic equation and introduced the heat flux into Levermore's 10 moment closures and obtained extended fluid dynamics equations for non-equilibrium flow simulation [6]. This new system leds to improved results in the transition flow regime where heat transfer has a significant effect. Other interesting research in this direction includes quasi-gas dynamic equations [7, 8].

Currently, the Direct Simulation Monte Carlo (DSMC) method is the most successful technique for numerical prediction of low density flows [9]. The DSMC method primarily consists of two steps, i.e., free transport and collision within each computational cell. The determination of the transport coefficients in the DSMC method is based on the particle collision model, which is based on the well-defined theories for continuum flows. The collision models for the particle cross section and the probability for each collision pair can be used for recovering the dissipative coefficients in the Navier-Stokes limit. For example, the commonly used variable hard sphere (VHS) molecular model in DSMC can be used to recover the first-order Chapman-Enskog expansion with viscosity coefficient $\mu = \mu_{ref}(T/T_{ref})^{\omega}$, which is of the Navier-Stokes order. However, when the DSMC method is used for non-equilibrium flow calculations, the particle transport from one place to another is controlled individually by each particle's velocity, which is not uniformly controlled by the macroscopically defined particle collision time τ, i.e., $\tau = \mu/p$, where μ is the dynamic viscosity coefficient and p is the pressure. Therefore, particle transport from one place to another in DSMC may be the key for capturing of non-equilibrium properties. Traditionally, it is noted that the concepts and measurements of the dissipative coefficients are limited to the continuum flow regime. A generalized mathematical formulation

of the stress and heat flux under rarefied flow conditions has not been developed so far. In order to construct valid macroscopic governing equations for non-equilibrium flow, instead of trying different kinds of approximate solutions of the Boltzmann equation, it may be important to borrow the critical ingredients of the DSMC method directly and use them in the construction of macroscopic equations.

In recent years, we have concentrated on the development of numerical schemes for near continuum flow simulation. To capture the non-equilibrium physics in the transitional flow regime, we have extended the gas-kinetic Navier-Stokes flow solver with the following developments [10]. First, a closed solution of the gas distribution function up to the NS order has been used to derive a generalized particle collision time to obtain the extended viscosity and heat conduction coefficients [11]. This step is mainly to mimic the effect of the transport process in the DSMC method. Later, in order to describe the non-equilibrium flow related to the molecular rotational and vibrational degree of freedom, a multiple time relaxation kinetic scheme was introduced for the shock structure calculations [12,13]. Recently, the gas-kinetic scheme was further extended to study the multiple translational temperature non-equilibrium [1]. The use of the multiple temperature in the above kinetic schemes is basically to incorporate the physical effect of the collision step in the DSMC method, where the pair collision in DSMC may not directly drive the system to equilibrium, but rather stay in an anisotropic middle state. The gas-kinetic schemes developed in the above study give reasonable results in the transitional flow regime, such as the capturing of shock structures at different Mach numbers and flow phenomena that cannot be described properly by the NS equations. In the above simulations, the underlying physical model is a generalized BGK (GBGK) model [1], where the multiple stage relaxation processes have been considered.

In gas-kinetic schemes, the solutions are obtained without knowing the explicit macroscopic governing equations. In this paper, we derive the underlying macroscopic governing equations for monatomic gas. In an earlier approach [1], we introduced the multiple translational temperature into the kinetic model, where the energy exchanges between the x-, y-, and z-directions are modeled through particle collisions. Based on the above kinetic model, in one-dimensional space, the generalized NS equations are derived, where the viscous term in the NS equations is replaced by the temperature relaxation term. In this paper, we further develop this model and regard the temperature as a second-order tensor. Since the gas flow may settle to an equilibrium state through multiple stages [14], one reasonable assumption is to use a Gaussian distribution with multiple temperature as a middle state. Physically, this state corresponds to a gas with different temperatures in different directions. Therefore, the thermal energy or particle random motion is represented through a symmetric temperature tensor, T_{ij}. Historically, the temperature has been defined as an equilibrium thermodynamic scalar variable. From the statistical physics, the clear physical meaning of the temperature is that it is mainly a Lagrangian multiplier under energy conservation constraint. In the transition flow regime, due to the long particle mean free path and insufficient particle collision, the local particle thermal energy will be effected from surrounding environment, such as different wall temperature in different directions. As a result, the energy constraints will depend on the spatial directions, so is the temperature. Therefore, in order to construct gas dynamic equations in the rarefied flow regime, to extend the temperature concept from a scalar to a tensor is justifiable. The commutable property of the random particle velocity determines the temperature to be a symmetric tensor. Actually, this kind of non-equilibrium gas property has been routinely extracted from DSMC solutions. Based on the physical model with the Gaussian distribution as a middle

state between the real gas distribution function, f, and the equilibrium Maxwellian, f^{eq}, and the strategy used in the construction of the kinetic scheme, we are going to derive the corresponding macroscopic governing equations. Surprisingly, the obtained gas dynamic equations become regularization of Levermore's 10 moment Gaussian closure, where additional viscous and heat conduction terms are obtained. The structure of the gas dynamic equations are almost identical to the Navier-Stokes equations, but the constitutive relationship of the NS which relates the stress tensor $\boldsymbol{\sigma}$ to the velocity gradient, i.e.,

$$\sigma_{ij} = -\rho RT^{eq}\delta_{ij} + \mu(\partial_i U_j + \partial_j U_i - \frac{2}{3}\partial_k U_k \delta_{ij}),$$

is replaced by a new relationship

$$\sigma_{ij} = -\rho RT_{ij} + \rho R(T_{ij}^{eq} - T_{ij}),$$

where T_{ij} is the temperature tensor. At the same time, the heat flux depends on the gradient of the temperature T_{ij}.

This paper is organized as follows. Section 2 introduces the kinetic equation and the generalized particle collision model. At the same time, the 10 moment closure and the generalized gas dynamics equations are presented. Section 3 presents applications of the new gas dynamics equations to two flow problems in the near continuum regime. Conclusions are drawn in section 4.

2. A Two Stage Gas-Kinetic Model

In this section, we will propose a gas kinetic model in which the collision process is approximated by a generalized BGK model. A monatomic gas is considered in this paper.

Our starting point is the standard Boltzmann equation for

$$\partial_t f + u_i \partial_i f = J(f, f), \tag{2.1}$$

where the particle distribution function, $f = f(\boldsymbol{x}, \boldsymbol{u}, t)$, is a function of time, t, spatial location, $\boldsymbol{x}$, and particle velocity, $\boldsymbol{u}$. The left-hand side of the above equation represents the free streaming of molecules in space, and the right-hand side, J, is the collision operator that describes the intermolecular interactions. Due to the complicated formulation of J, simplified models are usually employed to approximate the collision term. One widely used model is the so called Bhatnagar-Gross-Krook (BGK) model, in which the collision effect is modeled as a process that the non-equilibrium distribution function relaxes to its equilibrium state with a single rate, i.e.,

$$J = -\frac{1}{\tau}\left(f - f^{eq}\right), \tag{2.2}$$

where f^{eq} is the Maxwell equilibrium defined as

$$f^{eq} = \frac{\rho}{(2\pi RT^{eq})^{3/2}} \exp\left[-\frac{(u-U)^2}{2RT^{eq}}\right],$$

where ρ is the density, T^{eq} is the equilibrium temperature, and U_i is the averaged macroscopic fluid velocity, which are defined as the velocity moments of f:

$$\rho = \int f\, d\boldsymbol{u}, \quad \rho \boldsymbol{U} = \int \boldsymbol{u} f\, d\boldsymbol{u}, \quad \frac{3}{2}\rho RT^{eq} = \int \frac{(\boldsymbol{u}-\boldsymbol{U})^2}{2} f\, d\boldsymbol{u}. \tag{2.3}$$

Traditionally, based on the above BGK model, the Navier-Stokes and higher-order equations, such as the Burnett and the Super-Burnett, can be derived [16, 17]. Unfortunately, these higher-order equations have intrinsic physical and mathematical problems in the transitional flow regime. In general, the BGK collision term is valid only for flows close to the thermal equilibrium regime. To extend the capacity of the BGK model to the non-equilibrium flow regime, we spearate the total relaxation process to the equilibrium into two sub-processes. First, the non-equilibrium distribution function f relaxes to an intermediate state g between f and f^{eq}, and then g relaxes to the final equilibrium f^{eq} (see Fig. 1). This processes can be expressed as

$$J = -\frac{f-g}{\tau} - \frac{g-f^{eq}}{\tau}. \tag{2.4}$$

Although this model is identical to the BGK model mathematically, but the physical significance of two models is different. As indicated in Fig. 1, the present two-stage allows f to be far from the equilibrium state due to the middle state g, while the BGK model is intrinsically limited to near-equilibrium flows without such mechanism. The two-stage model (2.4) can also be generalized to use two relaxation times that characterizes the two sub-processes, i.e.,

$$J = -\frac{f-g}{\tau_1} - \frac{g-f^{eq}}{\tau_2}. \tag{2.5}$$

By adjusting τ_1 and τ_2, this generalized two-stage model can have an adjustable Prandtl number, while that given by Eq. (2.4) is fixed (i.e. $\Pr = 1$). However, the final macroscopic equations from both models have the same formulation and the Prandtl number can be easily fixed.

It is noted that the model (2.5) is similar to that given by Levermore [2, 23], in which the collision model is expressed as

$$J = -\frac{f-G}{\tau_a} - \frac{f-f^{eq}}{\tau_b}, \tag{2.6}$$

where G is a Gaussian distribution that is not necessarily equal to the intermediate state g used in the two-stage model (2.4) or (2.5). Actually, if we take $G = g$, $\tau_a = \tau_1$ and $\tau_b = (\tau_1\tau_2/(\tau_1+\tau_2))$, the two models are identical mathematically. However, the model of Levermore require $\tau_a \ll \tau_b$, but the present model has no such a limitation. Furthermore, the physical significance of Eq. (2.5) is different from that of Eq. (2.6). The former implies the relaxation process of a non-equilibrium is $f \to g \to f^{eq}$, i.e, the final state is still the equilibrium state; on the other hand, the latter implies that the non-equilibrium state relaxes to two different state, part to G and the others to f^{eq}.

Now we come to the definition of the intermediate state g. For the rarefied flow simulation, a generalized middle state can be a Gaussian distribution, which appears to have been derived in the early work by Maxwell [20], and then re-discovered by many researchers, such as Holway [21] and Levermore [2]. Since g is a middle state between f and f^{eq}, a natural choice is to assume that g is a Gaussian distribution with a second-order tensor T,

$$g(\rho, \boldsymbol{U}, \mathsf{T}) = \frac{\rho}{[\det(2\pi\mathsf{T})]^{1/2}} \exp\left[-\frac{1}{2}(\boldsymbol{u}-\boldsymbol{U})\cdot\mathsf{T}^{-1}\cdot(\boldsymbol{u}-\boldsymbol{U})\right], \tag{2.7}$$

where the T is defined as the average of the second-order moments of f and f^{eq},

$$T_{ij} = \frac{1}{\rho R}\int (u_i - U_i)(u_j - U_j)\frac{f+f^{eq}}{2}\,d\boldsymbol{u} = \frac{1}{2\rho R}\left(P_{ij} + \rho R T^{eq}\delta_{ij}\right), \tag{2.8}$$

where P_{ij} is the usual pressure tensor. In the present work, we call T as "temperature tensor" since it reflects the fluctuations of the gas molecules. It is obvious that

$$T^{eq} = \frac{1}{3}\mathrm{Tr}(T_{ij}) = \frac{1}{3}\mathrm{Tr}(P_{ij}/\rho R).$$

The intermediate state g defined by Eq. (2.7) is similar to the target state used in the Ellipsoidal Statistical BGK (ES-BGK) model [21], in which the collision model is defined as

$$J = -\frac{1}{\tau}\left[f - G_{ES}\right], \tag{2.9}$$

where the ES distribution function is defined as

$$G_{ES}(\rho, \boldsymbol{U}, \Gamma) = \frac{\rho}{[\det(2\pi\Gamma)]^{1/2}} \exp\left[-\frac{1}{2}(\boldsymbol{u}-\boldsymbol{U})\cdot\Gamma^{-1}\cdot(\boldsymbol{u}-\boldsymbol{U})\right], \tag{2.10}$$

with Γ being defined by $\rho R\Gamma_{ij} = \nu P_{ij} + (1-\nu)\rho R T^{eq}\delta_{ij}$. Here ν is a parameter to adjust the Prandtl number. Obviously, $g = G_{ES}$ as $\nu = 1/2$. However, the differences between the present two-stage model and the ES-BGK model are also apparent. First, the ES-BGK model is a one stage model, i.e., the target of the relaxation process is the ES state only defined by Eq. (2.10); while the second relaxation process in the present model enforce the final state to be a Maxwellian. Second, in the ES-BGK model ν is related to the Prandtl model, while in the present model the Prandtl number is free of the choice of g due to the introduction of the second stage. As can be seen later, the Prandtl number problem can be easily fixed in the present model.

In the two-stage collision model (2.4), the term $(f^{eq} - g)/\tau$ has no direct connection with f; therefore, we can consider it as a source term, and the generalized BGK (GBGK) model can be expressed as

$$\partial_t f + u_i \partial_i f = (g - f)/\tau + Q, \tag{2.11}$$

where $Q = (f^{eq} - g)/\tau$ for the monatomic gas.

We would like to note that the approximation of the Boltzmann particle collision term by multiple BGK-type sub-processes has been investigated before by many authors, such as Callaway [18], Gorban and Karlin [19], and Levermore [2]. In the DSMC method, the physical modeling of rotation and vibration is also through the BGK-type relaxation model. As realized in [2], for Maxwellian molecules, the use of the multiple BGK-type collision term is correct even if the flow is far away from the equilibrium. This suggests that the generalized BGK operator may be a legitimate approximation of the collision term for use in modeling non-equilibrium flows.

3. Generalized Gas Dynamic Equations

We now derive the hydrodynamic equations from the proposed two-stage kinetic model using an iteration method, which is different from the Chapman-Enskog multi-scale method. The initial distribution in the iteration process is assumed to be the intermediate state g, which gives the zeroth-order hydrodynamic equations which involve only first-order temporal and spatial derivatives; in the next order, the distribution function is expressed as the sum of g and a perturbation, and the resultant hydrodynamic equations contain second-order spatial derivatives.

3.1. Zeroth-order

In the zeroth-order, we assume $f = g$, the kinetic equation (2.11) then reduces to

$$\partial_t g + u_i \partial_i g = Q. \tag{3.1}$$

Taking the moments

$$\psi = (1, u_i, u_i u_j)^T,$$

on the above equation gives the following Gaussian closure:

$$\partial_t \rho + \partial_k(\rho U_k) = 0, \tag{3.2}$$

$$\partial_t(\rho U_i) + \partial_k[\rho(U_i U_k + RT_{ik})] = 0, \tag{3.3}$$

$$\partial_t[\rho(U_i U_j + RT_{ij})] + \partial_k[\rho(U_i U_j U_k + RU_k T_{ij} + RU_i T_{jk} + RU_j T_{ki})] = \frac{1}{\tau}\rho R(T^{eq}\delta_{ij} - T_{ij}). \tag{3.4}$$

These equations are actually the zeroth-order Chapman-Enskog expansion, i.e., $f = g$, for the generalized BGK model. In the above equations, the source term on the right-hand side comes from the term Q in the generalized BGK model. The equilibrium temperature, T^{eq}, is defined by

$$T^{eq} = \frac{1}{3}\mathrm{Tr}(T_{ij}).$$

If the state g is equal to the Maxwellian, i.e., $g = f^{eq}$, the above equations reduce to the Euler equations. It is noted that the structure of the above set of equations is similar to that of the Gaussian closure equations [2, 6, 23]. The only difference is that in Eqs. (3.3) and (3.4) the temperature tensor $\rho R\mathsf{T}$ is used while it is the pressure tensor P in the corresponding equations of the Gaussian closure model. The relation between the temperature and pressure tensor is given in Eq. (2.8). Based on the Gaussian closure moment equations, Levermore and Morokoff showed that if the initial data of P_{ij} is symmetric positive definite, then it remains so [22]. Due to the similar structures, T_{ij} should also persist this property.

In the Navier-Stokes equations, even though the stress tensor includes the non-equilibrium part, the temperature is still defined as a scalar function, which is used to describe the thermal energy of the Euler equations. The underlying assumption for this is that the random kinetic energy of particles is isotropic. In our model, we release the isotropic random energy assumption for the non-equilibrium flow. The thermal energy is direction-dependent and is described by a temperature tensor.

Furthermore, following the analysis in Ref. [2], it can be shown that the above set of equations, even without heat conduction terms, can recover the Navier-Stokes viscous terms in the continuum flow regime. In the above system, (3.2)-(3.4), the left-hand side equations have complete real eigenvalues and eigenvectors [23, 24], and the system is strictly hyperbolic. The temperature difference in different directions, such as the T_{ij}, basically shows that the speed of sound depends on the spatial direction, the so-called anisotropic wave propagation due to the non-isotropic gas property.

3.2. Generalized gas dynamic equations: first order

The generalized BGK model includes two relaxation processes. One is from f to the Gaussian, g, and the other is from g to an equilibrium state, f^{eq}. In the last section, the distribution

function f is assumed to be equal to g, and the 10 moment closure equations are derived. However, as presented in Fig. 1, the real distribution function should be different from g, and the process of relaxation from f to g must be considered. In the past years, we have developed gas-kinetic schemes based on the generalized BGK model, where a gas distribution function, f, around g has been constructed and used to evaluate the numerical fluxes in a finite volume scheme [1]. The schemes present reasonable numerical solutions in the near continuum flow regime, such as the micro-channel flow computation [14]. In the following, we derive the corresponding macroscopic governing equations underlying the gas-kinetic scheme. The method used here can be regarded as the Chapman-Enskog expansion or the iterative expansion [17]. They are equivalent.

The solution, f, around the Gaussian, g, is constructed using the iterative expansion to the first-order [17],

$$f = g - \tau(\partial_t g + u_i \partial_i g) + \tau Q, \tag{3.5}$$

where in the kinetic scheme, $\partial_t g$, is determined using the zeroth-order equations or the following compatibility condition

$$\int \psi(\partial_t g + u_i \partial_i g) du = \int \psi Q du, \tag{3.6}$$

which is exactly the 10 moment closure, (3.2)-(3.4). Substituting the distribution function, f, in (3.5) into the BGK model (2.11), the equation becomes

$$\partial_t g + u_i \partial_i g = \tau \left(\partial_t^2 g + 2u_i \partial_t \partial_i g + u_i u_j \partial_i \partial_j g\right) + Q - \tau \left(\partial_t Q + u_i \partial_i Q\right). \tag{3.7}$$

Taking the moments, ψ, of the above equation and using Eq. (3.6) to express the time derivative in terms of the spatial derivative, we have the following macroscopic equations:

$$\partial_t \rho + \partial_k(\rho U_k) = 0, \tag{3.8}$$

$$\partial_t(\rho U_i) + \partial_k[\rho(U_i U_k + RT_{ik})] = \partial_k[\rho R(T^{eq}\delta_{ki} - T_{ki})], \tag{3.9}$$

$$\begin{aligned}
&\partial_t[\rho(U_i U_j + RT_{ij})] + \partial_k[\rho(U_i U_j U_k + RU_k T_{ij} + RU_i T_{jk} + RU_j T_{ki})] \\
=&\frac{2}{\tau}\rho R(T^{eq}\delta_{ij} - T_{ij}) + \partial_k \{\rho R[U_k(T^{eq}\delta_{ij} - T_{ij}) + U_i(T^{eq}\delta_{jk} - T_{jk}) \\
&+ U_j(T^{eq}\delta_{ki} - T_{ki})]\} - \partial_k Q_{ijk},
\end{aligned} \tag{3.10}$$

where $\boldsymbol{Q}$ is the generalized heat flux given by

$$Q_{ijk} = -\frac{\tau\rho R^2}{\Pr}\left(T_{kl}\partial_l T_{ij} + T_{il}\partial_l T_{jk} + T_{jl}\partial_l T_{ki}\right). \tag{3.11}$$

Note that the BGK collision model give a unit Prandtl number Pr for the heat conduction term. However, since we believe that up to the NS order, the structure of the gas dynamic equations will not be changed due to the BGK collision term or the exact Boltzmann collision model, we add the Prandtl number in the above corresponding heat flux term. Theoretically, for the non-equilibrium flow the Prandtl number may not be a constant and will depend on direction as well. Since the viscosity and heat conduction coefficients are the concepts for the continuum flow, the particle collision time, τ, in the above equations is defined according to the result in the continuum regime,

$$\tau = \frac{\mu}{\rho R T^{eq}},$$

where μ is the dynamical viscosity coefficient. Certainly, in the rarefied flow regime, the corresponding viscosity coefficient has to be modified [11].

By making use of Eq. (2.8), we can rewrite Eqs. (3.9) and (3.10) as

$$\partial_t(\rho U_i) + \partial_k(\rho U_i U_k + P_{ik}) = 0, \tag{3.12}$$

$$\begin{aligned}&\partial_t[\rho(U_iU_j + RT_{ij})] + \partial_k[\rho U_iU_jU_k + U_kP_{ij} + U_iP_{jk} + U_jP_{ki})]\\ =&\frac{1}{\tau}\left(\rho RT^{eq}\delta_{ij} - P_{ij}\right) - \partial_k Q_{ijk}.\end{aligned} \tag{3.13}$$

Furthermore, the trace of Eq. (3.13) gives the conservation equation for the total energy as

$$\partial_t\left[\frac{1}{2}\rho U_iU_i + \frac{3}{2}\rho RT^{eq}\right] + \partial_k\left[\left(\frac{1}{2}\rho U_iU_i + \frac{5}{2}\rho RT^{eq}\right)U_k - \tau_{ik}U_i - \frac{1}{2}q_k\right] = 0, \tag{3.14}$$

where $q_k = -Q_{iik}$. It is clear that the continuity equation and momentum equations are the same as the 10 moment closure equations [2]. The difference is the heat conduction term Q_{ijk} which is absent in the 10 moment equation. This heat flux $\boldsymbol{Q}$ is similar to that obtained by McDonald and Groth, even though the equations are obtained given different considerations [6]. The Generalized heat flux by McDonald and Groth is obtained as a regularization of the 10-moment closure equation, which can be expressed as

$$Q'_{ijk} = -\frac{\tau}{\mathrm{Pr}}\left[P_{kl}\partial_l(P_{ij}/\rho) + P_{il}\partial_l(P_{jk}/\rho) + P_{jl}\partial_l(P_{ki}/\rho)\right]. \tag{3.15}$$

Since $P_{ij} \neq \rho RT_{ij}$ at nonequilibrium state, generally $Q_{ijk} \neq Q'_{ijk}$. This difference can be attributed to two main causes. First, the two-stage collision operator used in Eq. (2.4) is different from that for the model by McDonald and Groth [6] (i.e, the ES model); Second, in the derivation of the present model we used an iterative expansion while McDonald and Groth made use of the Chapman-Enskog expansion in their work.

The relaxation parameter, τ, controls the distance between the non-equilibrium state, f, and the equilibrium state, f^{eq}. The current method for the derivation of the gas dynamics equations can be used in other systems, such as one with a more complicated non-equilibrium middle state, g, such as the distributions with 14 or 26 moments. However, a distribution function, g, with higher-order terms may correspond to macroscopic governing equations without clear physical meanings for the higher-order terms.

The generalized gas dynamic equations, (3.8)-(3.10), have the same left-hand side as the 10 moment closure equations, (3.2)-(3.4) [22]. And the fluxes on the left have complete eigenvalues and eigenvectors [23–25]. In other words, the left-hand side is the hyperbolic part.

To gain a clear understanding of the difference between our model and the traditional Navier-Stokes equations, we can figure out the corresponding "NS" terms from the above equations (3.8)-(3.10). First, it is emphasized here that our equations basically represent a non-equilibrium system. The temperature tensor is different from the **pressure tensor** P_{ij}. Accordingly, the corresponding **viscous stress**, τ_{ij}, in our system becomes

$$\tau_{ij} = \frac{1}{3}P_{kk}\delta_{ij} - P_{ij} = 2\rho R(T^{eq}\delta_{ij} - T_{ij}).$$

As a result, the corresponding "NS" **stress tensor** σ_{ij} in our system, or the constitutive relationship, becomes

$$\sigma_{ij} = -\rho RT^{eq}\delta_{ij} + \tau_{ij} = -\rho RT_{ij} + \rho R(T^{eq}\delta_{ij} - T_{ij}). \tag{3.16}$$

In the following, we will show that the new constitutive relationship can recover the standard NS formulation in the continuum flow regime.

In the continuum flow regime, the Gaussian distribution, g, will come to the same state as the equilibrium one, f^{eq}, see Fig. 1. In this case, the first-order expansion of f presented in this section will be expanded basically around f^{eq}. To the leading order of small τ, Eq. (3.10) gives the temperature deviation,

$$\begin{aligned}&\rho R(T^{eq}\delta_{ij}-T_{ij})\\ \approx&\frac{\tau}{2}\bigg(\partial_t\left[\rho(U_iU_j+RT_{ij})\right]+\partial_k\left[\rho(U_iU_jU_k+RU_kT_{ij}+RU_iT_{jk}+RU_jT_{ki})\right]\bigg).\end{aligned}\tag{3.17}$$

In the above equation, when applying the equilibrium conditions, $T_{ii}=T^{eq}$ (no summation) and $T_{ij}=T^{eq}\delta_{ij}$, and using the Euler equations to replace the temporal derivative by the spatial derivative, we have

$$\begin{aligned}&\rho R(T^{eq}\delta_{ij}-T_{ij})\\ \approx&\frac{\tau}{2}\rho RT^{eq}\left(\partial_iU_j+\partial_jU_i-\frac{2}{3}\partial_kU_k\delta_{ij}\right)=\frac{\mu}{2}\left(\partial_iU_j+\partial_jU_i-\frac{2}{3}\partial_kU_k\delta_{ij}\right).\end{aligned}\tag{3.18}$$

Therefore, the constitutive relationship (3.16) becomes

$$\begin{aligned}\sigma_{ij}&=-\rho RT^{eq}\delta_{ij}+2\rho R(T^{eq}\delta_{ij}-T_{ij})\\ &=-p\delta_{ij}+\mu[\partial_iU_j+\partial_jU_i-\frac{2}{3}\partial_kU_k\delta_{ij}],\end{aligned}\tag{3.19}$$

which is exactly the Navier-Stokes stress-strain relationship. In the Navier-Stokes equations, the stress becomes the symmetric tensor, which is constructed through rational mechanical analysis. However, in the new gas dynamic equations, the "stress" tensor is automatically a symmetric tensor due to the commutable property of random particle velocities, i.e.,

$$(u_i-U_i)(u_j-U_j)=(u_j-U_j)(u_i-U_i).$$

In order words, the present formulation gives a microscopic interpretation of the origin of the symmetric stress tensor. At the same time, the heat flux transported in the $k-$direction for the thermal energy, ρRT_{ij}, becomes Q_{kij} defined by Eq. (3.11). These results are consistent with the early analysis of one-dimensional flow [1].

In summary, we derived generalized gas dynamics equations based on the multiple stage BGK model. With the added Prandtl number, Pr, and the introduction of dynamic viscosity in the determination of the relaxation parameter, τ, the gas dynamic equations derived in this section are a closed system, which is a natural extension of the Navier-Stokes equations. Theoretically, the new gas dynamic equations cover a wider flow regime than do the Navier-Stokes equations. The new constitutive relationship has a microscopic physical basis. The viscous term involves only first-order derivatives of the flow variables. The ability to treat non-equilibrium flow problems without evaluating higher than first-order derivatives would prove very advantageous numerically. The method should be insensitive to irregularities in the grid, the straight-forward computation in Discontinuous Galerkin framework, and the easy implementation of boundary conditions. Due to the low order equations, the less communication between the computational cells (small stencil) makes its numerical scheme more efficient to implement on parallel computing architecture.

4. Solutions of the Generalized Gas Dynamic Equations

In this section, we present two flow problems in the near continuum flow regime for the validation of the generalized gas dynamic equations derived in the last section. Both test problems are microchannel flows, but with different flow speeds and non-equilibrium properties.

4.1. Analytic solution of force-driven Poiseuille flow in the near continuum flow regime

In this subsection, we apply the generalized gas dynamic equations to rarefied gas flows, such as the case of a force-driven Poiseuille flow between two parallel plates. Both DSMC and kinetic theory have shown that even with a small Kn, the pressure and temperature profiles in this flow exhibit a different qualitative behavior from that predicted by the Navier-Stokes equations [26–31]. Therefore, this flow can serve as a good test problem for any extended hydrodynamic equations intended for non-continuum flow computation.

In our test, the two walls of the channel are located at $y = \pm H/2$ and the force, $\boldsymbol{a} = (a, 0, 0)$, is along the x-direction. The flow is assumed to be unidirectional, i.e., $\partial_x \phi = 0$, for any variable, ϕ, and the velocity has only an x-component in the laminar and stationary case, i.e., $\boldsymbol{U}_m = (U, 0, 0)$. Under such conditions, the generalized gas dynamic equations (3.8)-(3.10) reduce to

$$
\begin{aligned}
&2\frac{d\Theta_{xy}}{dy} - \rho a = 0, \quad \frac{d}{dy}(2\Theta_{yy} - P) = 0,\\
&\frac{1}{\mathrm{Pr}}\frac{d}{dy}\left(2\tau\Theta_{xy}\frac{d\theta_{xy}}{dy} + \tau\Theta_{yy}\frac{d\theta_{xx}}{dy}\right) = \frac{2(\Theta_{xx} - P)}{\tau} + 4\Theta_{xy}\frac{dU}{dy},\\
&\frac{3}{\mathrm{Pr}}\frac{d}{dy}\left(\tau\Theta_{yy}\frac{d\theta_{yy}}{dy}\right) = \frac{2(\Theta_{yy} - P)}{\tau},\\
&\frac{1}{\mathrm{Pr}}\frac{d}{dy}\left(\tau\Theta_{yy}\frac{d\theta_{zz}}{dy}\right) = \frac{2(\Theta_{zz} - P)}{\tau},\\
&\frac{1}{\mathrm{Pr}}\frac{d}{dy}\left(2\tau\Theta_{yy}\frac{d\theta_{xy}}{dy} + \tau\Theta_{xy}\frac{d\theta_{yy}}{dy}\right) = \frac{2\Theta_{xy}}{\tau} + (2\Theta_{yy} - P)\frac{dU}{dy},
\end{aligned}
$$

where $\Theta_{ij} = \rho\theta_{ij}$ and $P = \rho\theta$ is the pressure, with $\theta_{ij} = RT_{ij}$ and $\theta = RT^{eq}$.

It is difficult to obtain an analytical solution from the above nonlinear system. Here, we try to find an approximate solution using a perturbation method similar to that used in [28]. To this end, we first introduce the following dimensionless variables:

$$
\hat{y} = \frac{y}{H}, \quad \hat{\rho} = \frac{\rho}{\rho_0}, \quad \hat{\Theta}_{ij} = \frac{\Theta_{ij}}{P_0}, \quad \hat{\theta_{ij}} = \frac{\theta_{ij}}{\theta_0}, \quad \hat{U} = \frac{U}{\sqrt{\theta_0}}, \quad \hat{\tau} = \frac{\tau}{\tau_0},
$$

where the variables with subscript 0 represent the corresponding reference quantities. With these dimensionless variables, the system can be rewritten as

$$
\frac{d\hat{\Theta}_{xy}}{d\hat{y}} - \epsilon\hat{\rho} = 0, \tag{4.1}
$$

$$
2\hat{\Theta}_{yy} - \hat{P} = C, \tag{4.2}
$$

$$
\frac{d}{d\hat{y}}\left(2\hat{\tau}\hat{\Theta}_{xy}\frac{d\theta_{xy}}{d\hat{y}} + \hat{\tau}\hat{\Theta}_{yy}\frac{d\hat{\theta}_{xx}}{d\hat{y}}\right) = 2\mathrm{Pr}\delta^2\frac{(\hat{\Theta}_{xx} - P)}{\tau} + 4\mathrm{Pr}\delta\hat{\Theta}_{xy}\frac{d\hat{U}}{d\hat{y}}, \tag{4.3}
$$

$$\frac{d}{d\hat{y}}\left(\hat{\tau}\hat{\Theta}_{yy}\frac{d\hat{\theta}_{yy}}{d\hat{y}}\right)=2\mathrm{Pr}\delta^2\frac{(\hat{\Theta}_{yy}-\hat{P})}{\tau}, \tag{4.4}$$

$$\frac{d}{d\hat{y}}\left(\hat{\tau}\hat{\Theta}_{yy}\frac{d\hat{\theta}_{zz}}{d\hat{y}}\right)=2\mathrm{Pr}\delta^2\frac{(\hat{\Theta}_{zz}-\hat{P})}{\tau}, \tag{4.5}$$

$$\frac{d}{d\hat{y}}\left(2\hat{\tau}\hat{\Theta}_{yy}\frac{d\hat{\theta}_{xy}}{d\hat{y}}+\hat{\tau}\hat{\Theta}_{xy}\frac{d\hat{\theta}_{yy}}{d\hat{y}}\right)=2\mathrm{Pr}\delta^2\frac{\hat{\Theta}_{xy}}{\tau}+C\mathrm{Pr}\delta\frac{d\hat{U}}{d\hat{y}}, \tag{4.6}$$

where C is a constant, ϵ and δ are two dimensionless parameters given by

$$\epsilon=\frac{a}{2\theta_0},\quad \delta=\frac{H}{\tau_0\sqrt{\theta_0}}=\sqrt{\frac{\pi}{2}}\frac{1}{\mathrm{Kn}}.$$

Now, we assume that the force acceleration, a, is small, such that $\epsilon\ll 1$. Then, we can expand the dimensionless flow quantities by powers of $\hat{\epsilon}$ (we will omit the hat for simplicity hereafter):

$$\begin{aligned}
&\rho=1+\epsilon^2\rho^{(2)}+\mathcal{O}(\epsilon^4),\quad U=\epsilon U^{(1)}+\mathcal{O}(\epsilon^3),\quad C=1+\epsilon^2C^{(2)},\\
&\Theta_{xy}=\epsilon\Theta_{xy}^{(1)}+\mathcal{O}(\epsilon^3),\quad \theta_{xy}=\epsilon\theta_{xy}^{(1)}+\mathcal{O}(\epsilon^3),\\
&\Theta_{ii}=1+\epsilon^2\Theta_{ii}^{(2)}+\mathcal{O}(\epsilon^4),\quad \theta_{ii}=1+\epsilon^2\theta_{ii}^{(2)}+\mathcal{O}(\epsilon^4),\quad \text{for}\quad i=x,y,z,\\
&P=1+\epsilon^2P^{(2)}+\mathcal{O}(\epsilon^4),\quad \theta=1+\epsilon^2\theta^{(2)}+\mathcal{O}(\epsilon^4),\quad \tau=1+\epsilon^2\tau^{(2)}+\mathcal{O}(\epsilon^4).
\end{aligned}$$

The odd or even properties of the variables as functions of ϵ are based on their symmetric properties in terms of the acceleration a. In general, the odd (even) velocity moments of the distribution function, f, are also odd (even) functions of ϵ. Furthermore, from the definition $\Theta_{ij}=\rho\theta_{ij}$ we can obtain some useful relations that will be used later:

$$\rho^{(2)}=P^{(2)}-\theta^{(2)}=\Theta_{ii}^{(2)}-\theta_{ii}^{(2)},\quad \Theta_{xy}^{(1)}=\theta_{xy}^{(1)},\quad \text{for}\quad i=x,y,z. \tag{4.7}$$

By substituting the above expansions into the nondimensional system, we obtain the first-order differential equation in ϵ. Eqs. (4.1) and (4.6) become

$$\begin{aligned}
&\frac{d\Theta_{xy}^{(1)}}{dy}-1=0,\\
&\mathrm{Pr}\delta\frac{dU^{(1)}}{dy}=\frac{d^2\theta_{xy}^{(1)}}{dy^2}-2\mathrm{Pr}\delta^2\Theta_{xy}^{(1)},
\end{aligned}$$

which give

$$\Theta_{xy}^{(1)}=\theta_{xy}^{(1)}=y, \tag{4.8}$$

$$U^{(1)}=-\delta y^2+C', \tag{4.9}$$

where C' is a constant. Here, we have made use of the symmetry of the velocity profile about $y=0$. From Eqs. (4.2)-(4.4), we can obtain the second-order equations in ϵ:

$$2\Theta_{yy}^{(2)}-P^{(2)}=C^{(2)}, \tag{4.10}$$

$$\frac{d^2\theta_{xx}^{(2)}}{dy^2}=2\mathrm{Pr}\delta^2\left(\theta_{xx}^{(2)}-\theta^{(2)}\right)-1-8\mathrm{Pr}\delta^2y^2, \tag{4.11}$$

$$3\frac{d^2\theta_{yy}^{(2)}}{dy^2}=2\mathrm{Pr}\delta^2\left(\theta_{yy}^{(2)}-\theta^{(2)}\right), \tag{4.12}$$

$$\frac{d^2\theta_{zz}^{(2)}}{dy^2} = 2\mathrm{Pr}\delta^2\left(\theta_{zz}^{(2)} - \theta^{(2)}\right), \tag{4.13}$$

where the results up to the first-order Eqs. (4.8) and (4.9) have been used. Summing up the above three equations, we have

$$\frac{d^2}{dy^2}\left(3\theta^{(2)} + 2\theta_{yy}^{(2)}\right) = -1 - 8\mathrm{Pr}\delta^2 y^2. \tag{4.14}$$

From Eqs. (4.12) and (4.14), we have

$$\theta^{(2)} = -\frac{2}{3}A\cosh\left(\frac{\sqrt{10}}{3}Ky\right) - \frac{2K^2}{15}y^4 + \frac{43}{50}y^2 + \frac{231}{125K^2} + B,$$

$$\theta_{yy}^{(2)} = A\cosh\left(\frac{\sqrt{10}}{3}Ky\right) - \frac{2K^2}{15}y^4 - \frac{77}{50}y^2 - \frac{693}{250K^2} + B,$$

where $K = \sqrt{\mathrm{Pr}}\delta$, A and B are two integral constants dependent on boundary or other conditions. Since $\theta^{(2)}$ is obtained, the other two temperatures, $\theta_{xx}^{(2)}$ and $\theta_{zz}^{(2)}$, from Eqs. (4.11) and (4.13) can be constructed, respectively.

Now, let us find the second-order pressure, $P^{(2)}$. From Eqs. (4.7) and (4.10), we obtain

$$P^{(2)} = C^{(2)} + 2(\theta^{(2)} - \theta_{yy}^{(2)}) = C^{(2)} - \frac{10A}{3}\cosh\left(\frac{\sqrt{10}}{3}Ky\right) + \frac{24}{5}y^2 + \frac{231}{25K^2}.$$

Then, $\rho^{(2)}$ can be determined from (4.7) as

$$\rho^{(2)} = P^{(2)} - \theta^{(2)} = C^{(2)} - \frac{8A}{3}\cosh\left(\frac{\sqrt{10}}{3}Ky\right) + \frac{2K^2}{15}y^4 + \frac{197}{50}y^2 + \frac{924}{125K^2} - B.$$

To summarize, the second-order perturbation coefficients can be expressed as

$$\theta^{(2)} = C_0\cosh\left(\frac{\sqrt{10}}{3}Ky\right) - \frac{2K^2}{15}y^4 + \frac{43}{50}y^2 + C_1, \tag{4.15}$$

$$P^{(2)} = 5C_0\cosh\left(\frac{\sqrt{10}}{3}Ky\right) + \frac{24}{5}y^2 + \frac{231}{25K^2} + C_2, \tag{4.16}$$

$$\rho^{(2)} = 4C_0\cosh\left(\frac{\sqrt{10}}{3}Ky\right) + \frac{2K^2}{15}y^4 + \frac{197}{50}y^2 + C_2 - C_1, \tag{4.17}$$

where C_0, C_1, and C_2 are constants dependent on boundary conditions. With the above results, we finally get the approximate solutions of the problem:

$$\frac{U}{\sqrt{RT_0}} = -\epsilon\delta\left(\frac{y}{H}\right)^2 + U_s, \quad \frac{P}{P_0} = 1 + \epsilon^2 P^{(2)}, \quad \frac{T}{T_0} = 1 + \epsilon^2\theta^{(2)}, \tag{4.18}$$

where U_s is the non-dimensional slip velocity at the wall.

With these results, we are able to discuss the velocity, pressure, and temperature profiles for the force-driven Poiseuille flow problem. First, it is clear that the velocity profile is parabolic, but the profiles of pressure and temperature may be complicated due to the presence of the hyperbolic cosine function.

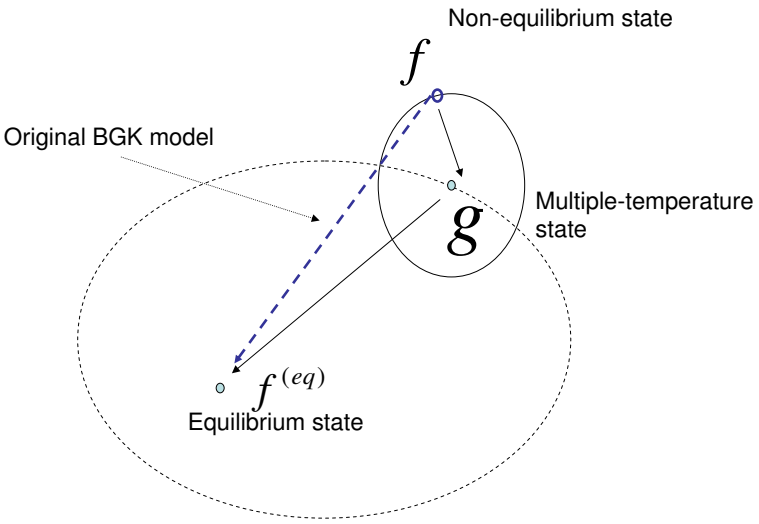

Fig. 4.1. Schematic representation of particle collision relaxation processes.

It is interesting to compare the approximate solutions of the present gas dynamic equations to those of the Navier-Stokes-Fourier (NSF) equations. For the same flow problem, the NSF equations reduce to

$$\frac{d}{dy}\left(\mu\frac{dU}{dy}\right)+\rho a=0, \tag{4.19}$$

$$\frac{dP}{dy}=0, \tag{4.20}$$

$$\frac{d}{dy}\left(k\frac{dU}{dy}\right)+\mu\left(\frac{dU}{dy}\right)^2=0. \tag{4.21}$$

Using the similar perturbation method, we have the following approximate solutions for the NSF equations:

$$\frac{U}{\sqrt{RT_0}}=-\epsilon\delta\left(\frac{y}{H}\right)^2+U_s,\quad P=\text{const},\quad \frac{T}{T_0}=1+\epsilon^2\theta^{(2)}_{nsf}, \tag{4.22}$$

where $\theta^{(2)}_{nsf}=-(2/15)\text{Pr}\delta^2\hat{y}^4+D$ and D is a constant. It is shown that the velocity profile of the NSF equations is also parabolic, which is the same as the that of the generalized hydrodynamic equations. However, the NSF equations give a constant pressure, which is qualitatively different from the predictions of the new proposed model. For the temperature, it is evident that $\theta^{(2)}_{nsf}$ is only part of $\theta^{(2)}$, and has one local maximum at $y=0$. On the other hand, the presence of terms, $\cosh(y)$ and y^2, in $\theta^{(2)}$ of the new model makes it possible to have a local minimum at $y=0$, due to

$$[\theta^{(2)}]'_{y=0}=0\quad\text{and}\quad[\theta^{(2)}]''_{y=0}=-K^2(100A+216)/135+1.72>0$$

as $A<2.322K^{-2}-2.16$.

To see this more clearly, we present the pressure and temperature profiles for the case of Kn=0.1 which was studied extensively using the DSMC method [30]. The constants A and

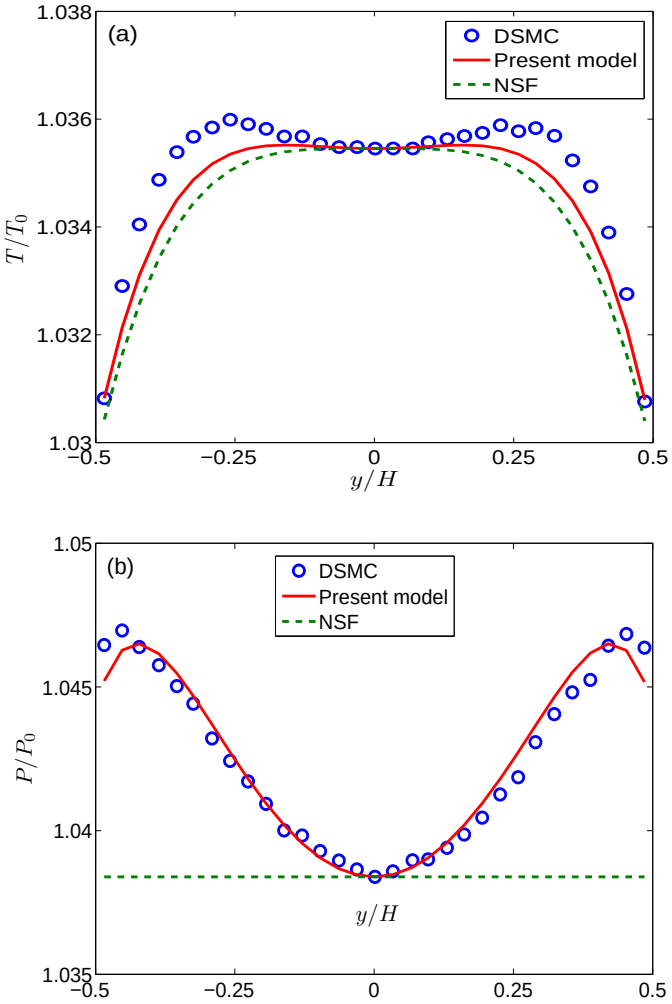

Fig. 4.2. Temperature (a) and pressure (b) at $Kn = 0.1$, where the results from the DSMC [30], the present model, and the Navier-Stokes-Fourier (NSF) model are presented.

B in θ and P of the present hydrodynamic model are obtained by enforcing the values of θ at $y = 0$ and $-H/2$ to be the same as the DSMC data, and then C is obtained by enforcing $P(y = 0)$ to be the DSMC value. The NSF solutions are obtained by enforcing their pressure and temperature values to be identical to the DSMC data at $y = 0$. In Fig. 4.2, the reduced temperature and pressure variations,

$$\theta^{(2)} = (T/T_0 - 1)/\epsilon^2 \quad \text{and} \quad P^{(2)} = (P/P_0 - 1)/\epsilon^2,$$

are shown for both the NSF equations and the present model. It is seen that the temperature and pressure profiles of the present model are in qualitative agreement with the DSMC data. For example, the temperature has a bimodal shape and exhibits a local minimum at $y = 0$, and the pressure has two local maximums near the two walls. These critical flow behaviors are absent in the profiles of the NSF equations. For example, the temperature minimum only appears in the super-Burnett order if the traditional BGK collision model is used to construct

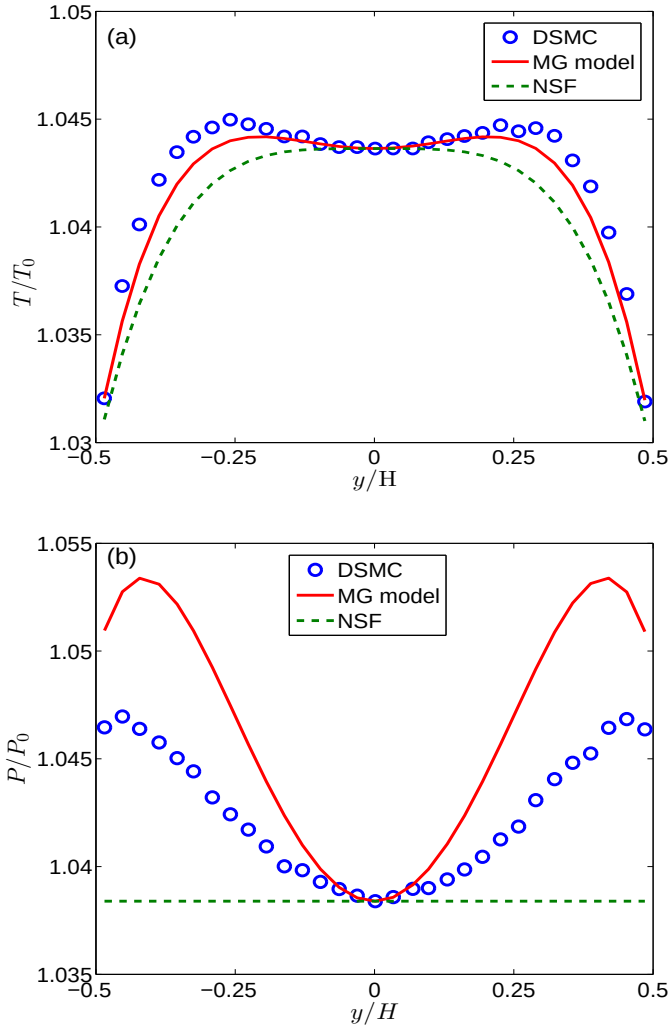

Fig. 4.3. Temperature (a) and pressure (b) at $Kn = 0.1$, where the results from the DSMC [30], the regularized 10-moment (MG) model [6], and the Navier-Stokes-Fourier (NSF) model are presented.

the gas dynamic equations [16,32]. These observations demonstrate the fundamental difference between the present hydrodynamic model and the NSF equations.

We would also like to point out that the original Gaussian moment equations [2] cannot be used to describe the structure of the force-driven Poiseuille flow due to the absence of the conduction terms in the energy equation. Actually, for the Poiseuille flow the 10 moment equations reduce to

$$\frac{dP_{xy}}{dy} - \rho a = 0, \tag{4.23}$$

$$\frac{dP_{yy}}{dy} = 0, \tag{4.24}$$

$$\frac{(P_{xx} - P)}{\tau} + 2P_{xy}\frac{dU}{dy} = 0, \tag{4.25}$$

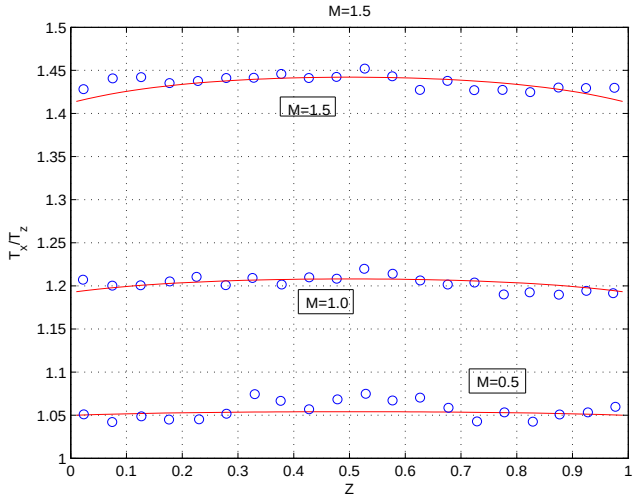

Fig. 4.4. The ratio of the temperature components, T_x/T_z, in relation to the vertical position, $Z = z/h_0$, in a planar Couette flow for Knudsen number Kn=1.25, and Mach numbers $M = 0.5, 1.0$, and 1.5. The solid lines are the solutions of the new gas dynamic equations and the circles are the DSMC solutions [33].

$$\frac{(P_{yy} - P)}{\tau} = 0, \tag{4.26}$$

$$\frac{(P_{zz} - P)}{\tau} = 0, \tag{4.27}$$

$$\frac{P_{xy}}{\tau} + P_{yy}\frac{dU}{dy} = 0, \tag{4.28}$$

The first equation indicates that $P_{xy} \neq 0$, while Eqs. (4.25), (4.24), and (4.27) give that

$$P_{xx} = P_{yy} = P_{zz} = P \quad \text{and} \quad P_{xy}\frac{dU}{dy} = 0,$$

which means that U must be a constant. One the other hand, the last equation, (4.28) means that U cannot be a constant. This contradiction reveals the insufficiency of the Gaussian closure for flows undergoing thermal diffusion.

We have also made a similar analysis for the regularized 10-moment model by McDonald and Groth [6] (MG model). The final perturbation solutions of the system are given as follows:

$$\theta^{(2)} = C_0 \cosh\left(\frac{\sqrt{10}}{6}Ky\right) - \frac{2K^2}{15}y^4 + \frac{86}{25}y^2 + C_1,$$

$$P^{(2)} = 5C_0 \cosh\left(\frac{\sqrt{10}}{6}Ky\right) + \frac{96}{5}y^2 + C_2.$$

where C_0, C_1, and C_2 are integral constants. It is clear from the above solutions that the flow structures predicted by the MG model is similar to that of the present hydrodynamic model. This can also be seen obviously from Fig. 4.3 where the integral constants are determined as before. By Comparing with Fig. 4.2, it can be observed that the temperature profile of the MG model agrees with the DSMC data slightly better than the present model, while the pressure profile does slightly worse.

4.2. Numerical solution for Couette flows

For the new gas dynamic equations, a corresponding gas-kinetic scheme can be developed [1]. To test the validity of the new governing equations, we study a planar Couette flow [33]. The height of the Couette system is $h_0 = 50\ nm$. The wall's temperatures are fixed at $T_0 = 273K$ and, at equilibrium, the pressure of the gas is 1 atm. Given that the distance between walls is less than a mean-free path and the relative wall speed is high, the gas system will be strongly out of equilibrium. Specifically, the velocity distribution for the particles is non-Maxwellian. As in [33], the temperature along the channel is defined as T_x and the temperature perpendicular to walls is T_z. With the fixed Knudsen number Kn= 1.25, and various wall velocities, such as the Mach numbers $M = 0.5, 1.0$, and 1.5, the simulation results from the new gas dynamic equations are shown in Fig. 4.4, where the DSMC solutions are also included [33]. Clearly, at high Knudsen number and Mach numbers, the temperature is anisotropic. The new gas dynamics equations are capable of capturing this kind of non-equilibrium flow phenomena. Also, it is necessary for any gas dynamic equations to consider the temperature as a tensor for the non-equilibrium system.

5. Conclusion

Based on the multiple stage particle collision BGK model and the Gaussian distribution function as the middle state, the generalized gas dynamic equations have been derived. Since the gas temperature basically represents the molecular random motion, the direct extension of the temperature concept from a scalar to a second-order symmetric tensor, T_{ij}, is reasonable. In the statistical physics, the physical meaning of the temperature is a Lagrangian multiplier under energy conservation constraint. In the rarefied flow regime, local particles random energy will depend on the directions where the particles are coming from. As a result, the energy constraints can depend on spatial directions, so is the temperature. The new gas dynamic equations have the same structure as the Navier-Stokes equatons, but the NS constitutive relationship,

$$\sigma_{ij} = -\rho R T^{eq}\delta_{ij} + \mu\left(\partial_i U_j + \partial_j U_i - \frac{2}{3}\partial_k U_k \delta_{ij}\right)$$

is replaced by

$$\sigma_{ij} = -\rho R T_{ij} + \rho R(T^{eq}\delta_{ij} - T_{ij}).$$

At the same time, the heat flux in the $k-$direction for the transport of thermal energy, $\rho R T_{ij}$, becomes

$$Q_{kij} = -\frac{\tau \rho R^2}{\Pr}\left(T_{kl}\partial_l T_{ij} + T_{il}\partial_l T_{jk} + T_{jl}\partial_l T_{ki}\right).$$

In the continuum flow regime, the generalized constitutive relationship and the heat flux term are the corresponding Navier-Stokes formulations. The new gas dynamic equations can be regarded as a regularization of Levermore's 10 moment closure equations [2]. The gas dynamic equations have a wider applicable flow regime than that of the NS equations. They capture the time evolution of the anisotropic non-equilibrium flow variables, as demonstrated in our examples.

The traditional temperature concept come from equilibrium thermodynamics, in which there is no anisotropic particle random motion in space. However, for the non-equilibrium flow transport, due to inadequate particle collisions the random molecule motion can become easily anisotropic. To directly consider the temperature as a tensor rather than a scalar is a reasonable

description of a non-equilibrium flow. For a diluted gas, due to the lack of long-range particle interactions, the randomness of the particle motion is the only source for the dissipation in the system. Under the new definition of the temperature, all dissipative effects in a diluted gas system, such as the viscosity and heat conduction, can be unified under the same concept, T_{ij}. The introduction of anisotropic Gaussian in the ES-BGK model is mainly for the modification of Prandtl number. Here, we explicitly present the anisotropic temperature concept, which is used to describe the physical reality, such as those routinely observed in the DSMC simulations. The current gas dynamic equations can be useful in the study of non-equilibrium flows in the near continuum flow regime. In the current generalized gas dynamic equations, the total thermal energy is invariant with respect to the system of coordinates. However, the individual temperature seems depend on the coordinate system, which deserves further investigation.

Finally, it should be pointed out that the Boltzmann equation can be also directly applied to the current multiple stage gas evolution model to derive its corresponding macroscopic governing equations. Instead of the Chapman-Enskog expansion around a Maxwellian, the same expansion can be also used around a multiple temperature Gaussian as well, and this multiple temperature Gaussian will automatically goes back to the Maxwellian in the continuum flow regime.

Acknowledgments. K. Xu would like to thank Prof. C. Groth and Mr. J.G. McDonald for helpful discussion and Dr. H.W. Liu for his help in the numerical testing of Couette flow. This research was supported by Hong Kong Research Grants Council 621709, National Natural Science Foundation of China (Project No. 10928205), National Key Basic Research Program (2009CB724101). Z. Guo acknowledges support from the National Natural Science Foundation of China (50721005) and the Program for NCET in University (NCET-07-0323).

Appendix

Gas Dynamic Equations in 2D Space

As a special application, we consider the 2D case, where there are seven unknowns (ρ, U, V, T_{xx}, T_{xy}, T_{yy}, T_{zz}). The generalized gas dynamic equations for those unknowns are

$$\frac{\partial \mathbf{U}}{\partial t} + \frac{\partial \mathbf{F}}{\partial x} + \frac{\partial \mathbf{G}}{\partial y} = \frac{\partial \mathbf{E_v}}{\partial x} + \frac{\partial \mathbf{F_v}}{\partial y} + \mathbf{S},$$

where $\mathbf{U}$ is the vector macroscopic flow variable, and $\mathbf{F}$ and $\mathbf{G}$ are $x-$ and $y-$direction flux vectors given by

$$\mathbf{U} = \begin{pmatrix} \rho \\ \rho U \\ \rho V \\ \rho(U^2 + RT_{xx}) \\ \rho(UV + RT_{xy}) \\ \rho(V^2 + RT_{yy}) \\ \rho RT_{zz} \end{pmatrix}, \quad \mathbf{F} = \begin{pmatrix} \rho U \\ \rho(U^2 + RT_{xx}) \\ \rho(UV + RT_{xy}) \\ \rho(U^3 + 3URT_{xx}) \\ \rho(U^2V + 2URT_{xy} + VRT_{xx}) \\ \rho(UV^2 + URT_{yy} + 2VRT_{xy}) \\ \rho URT_{zz} \end{pmatrix},$$

$$\mathbf{G}=\begin{pmatrix}\rho V\\ \rho(UV+RT_{xy})\\ \rho(V^2+RT_{yy})\\ \rho(U^2V+VRT_{xx}+2URT_{xy})\\ \rho(UV^2+URT_{yy}+2VRT_{xy})\\ \rho(V^3+3VRT_{yy})\\ \rho VRT_{zz}\end{pmatrix},$$

$$\mathbf{E_v}=\begin{pmatrix}0\\ \rho R(T^{eq}\delta_{xx}-T_{xx})\\ \rho R(T^{eq}\delta_{xy}-T_{xy})\\ 3\rho R[U(T^{eq}\delta_{xx}-T_{xx})+\tau R(T_{xx}\partial_xT_{xx}+T_{xy}\partial_yT_{xx})]\\ \rho R[V(T^{eq}\delta_{xx}-T_{xx})+2U(T^{eq}\delta_{xy}-T_{xy}+\tau R(T_{xy}\partial_xT_{xx}+T_{yy}\partial_yT_{xx}+2T_{xx}\partial_xT_{xy}+2T_{xy}\partial_yT_{xy}))]\\ \rho R[U(T^{eq}\delta_{yy}-T_{yy})+2V(T^{eq}\delta_{xy}-T_{xy})+\tau R(2T_{xy}\partial_xT_{xy}+2T_{yy}\partial_yT_{xy}+T_{xx}\partial_xT_{yy}+T_{xy}\partial_yT_{yy})]\\ \rho R[U(T^{eq}\delta_{zz}-T_{zz})+\tau R(T_{xx}\partial_xT_{zz}+T_{xy}\partial_yT_{zz})]\end{pmatrix},$$

$$\mathbf{F_v}=\begin{pmatrix}0\\ \rho R(T^{eq}\delta_{xy}-T_{xy})\\ \rho R(T^{eq}\delta_{yy}-T_{yy})\\ \rho R[V(T^{eq}\delta_{xx}-T_{xx})+2U(T^{eq}\delta_{xy}-T_{xy})+\tau R(2T_{xy}\partial_yT_{xy}+2T_{xx}\partial_xT_{xy}+T_{yy}\partial_yT_{xx}+T_{xy}\partial_xT_{xx})]\\ \rho R[U(T^{eq}\delta_{yy}-T_{yy})+2V(T^{eq}\delta_{xy}-T_{xy}+\tau R(T_{xy}\partial_yT_{yy}+T_{xx}\partial_xT_{yy}+2T_{yy}\partial_yT_{xy}+2T_{xy}\partial_xT_{xy}))]\\ 3\rho R[V(T^{eq}\delta_{yy}-T_{yy})+\tau R(T_{yy}\partial_yT_{yy}+T_{xy}\partial_xT_{yy})]\\ \rho R[V(T^{eq}\delta_{zz}-T_{zz})+\tau R(T_{yy}\partial_yT_{zz}+T_{xy}\partial_xT_{zz})]\end{pmatrix},$$

and the source term is

$$\mathbf{S}=\begin{pmatrix}0\\ 0\\ 0\\ 2\rho R(T^{eq}\delta_{xx}-T_{xx})/\tau\\ 2\rho R(T^{eq}\delta_{xy}-T_{xy})/\tau\\ 2\rho R(T^{eq}\delta_{yy}-T_{yy})/\tau\\ 2\rho R(T^{eq}\delta_{zz}-T_{zz})/\tau\end{pmatrix},$$

In the above equations, the equilibrium temperature is

$$T^{eq}=T^{eq}\delta_{xx}=T^{eq}\delta_{yy}=T^{eq}\delta_{zz}=\frac{1}{3}\mathrm{tr}(T_{ij}),$$

where $T^{eq}\delta_{xy}=T^{eq}\delta_{yx}=0$.

References

[1] K. Xu, H. Liu and J. Jiang, Multiple temperature kinetic model for continuum and near continuum flows, *Phys. Fluids*, **19** (2007), 016101.

[2] C.D. Levermore, Moment closure hierarchies for kinetic theories, *J. Stat. Phys.*, **83** (1996), 1021-1065.
[3] H. Grad, On the kinetic theory of rarefied gases, *Commun. Pur. Appl. Math.*, **2** (1949), 331-407.
[4] H. Struchtrup and M. Torrilhon, Regularization of Grad's 13 moment equations: derivation and linear analysis, *Phys. Fluids*, **15** (2003), 2668-2680.
[5] C.P.T. Groth, P.L. Roe, T.I. Gombosi, S.L. Brown, On the nonstationary wave structure of a 35-moment closure for rarefied gsa dynamics, paper AIAA 95-2312 (1995).
[6] J.G. McDonald and C.P.T. Groth, Extended fluid-dynamic model for micron-scale flows based on Gaussian moment closure, paper AIAA 2008-691 (2008).
[7] T.G. Elizarova, Quasi-Gas Dynamic Equations, Springer, 2009.
[8] T.G. Elizarova, J.C. Lengrand, I.A. Graur, Gradient expansions for distribution functions and derivation of moment equations, *21th Intern. Symp.on Rarefied Gas Dynamics*, Marseille, France, July 26-30 (1998) (paper 2057).
[9] G.A. Bird, Molecular gas dynamics and the direct simulation of gas flows, *Clarendon Press, Oxford*, (1994).
[10] K. Xu, A gas-kinetic BGK scheme for the Navier-Stokes equations and its connection with artificial dissipation and Godunov method, *J. Comput. Phys.*, **171** (2001), 289–335.
[11] K. Xu, Regularization of the Chapman-Enskog expansion and its description of shock structure, *Phys. Fluids*, **14** (2002), L17.
[12] K. Xu and E. Josyula, Continuum formulation for non-equilibrium shock structure calculation, *Commun. Comput. Phys.*, **1** (2006), 425-450.
[13] C.P. Cai, D. Liu, and K. Xu, A one-dimensional multiple-temperature gas-kinetic BGK scheme for shock wave computation, *AIAA J*, **46**:5 (2008), 1054-1062.
[14] K. Xu, A generalized Bhatnagar-Gross-Krook model for non-equilibrium flows, *Phys. Fluids*, **20** (2008), 026101.
[15] P. L. Bhatnagar, E. P. Gross, and M. Krook, A model for collision processes in gases. I: Small amplitude processes in charged and neutral one-component systems, *Phys. Rev.*, **94** (1954), 511–525.
[16] S. Chapman and T. G. Cowling, The Mathematical Theory of Non-Uniform Gases, Cambridge University Press, Cambridge, 1971.
[17] T. Ohwada and K. Xu, The kinetic scheme for full Burnett equations, *J. Comput. Phys.*, **201** (2004), 315-332.
[18] J. Callaway, Model for lattice thermal conductivity at low temperature, *Phy. Rev.*, **113** (1959), 1046-1051.
[19] A.N. Gorban and I.V. Karlin, General approach to constructing model of the Boltzmann equation, *Phyica A*, **206** (1994), 401-420.
[20] J.C. Maxwell, On the dynamical theory of gases, *Philosophical Transactions of Royal Society of London*, **157** (1867), 49-88.
[21] L.H. Holway, New statistical models for kinetic theory: methods of construction, *Phys. fluids*, **9** (1966), 1658-1673.
[22] C.D. Levermore and W.J. Morokoff, The Gaussian moment closure for gas dynamics, *SIAM J. Appl. Math.*, **59** (1998), 72-96.
[23] Shawn L. Brown, Approximate Riemann Solvers for Moment Models of Dilute Gases, *PhD Thesis* at Aerospace Engineering Department, University of Michigan (1996).
[24] J.A. Hittinger, Foundations for the Generalization of the Godunov Method to Hyperbolic Systems with Stiff Relxation Source Terms, *PhD Thesis* at Aerospace Engineering Department, University of Michigan (2000).
[25] J.G. McDonald, Numerical Modeling of Micron-Scale Flows using the Gaussian Moment Closure, *Master Thesis* at Department of Aerospace Engineering, University of Toronto (2005).
[26] M. M. Malek, F. Baras, and A. L. Garcia, On the validity of hydrodynamics in plane Poiseuille

flows, *Physica A*, **240** (1997), 255.
[27] M. Tij and A. Santos, Perturbation analysis of a stationary nonequilibrium flow generated by an external force, *J. Stat. Phys.*, **76** (1994), 1399.
[28] M. Tij, M. Sabbane, and A. Santos, Nonlinear Poiseuille flow in a gas, *Phys. Fluids*, **10** (1998), 1021.
[29] K. Aoki, S. Takata, and T. Nakanishi, Poiseuille-type flow of a rarefied gas between two parallel plates driven by a uniform external force, *Phys. Rev. E*, **65** (2002), 026315.
[30] Y. Zheng, A.L. Garcia, and B.J. Alder, Comparison of Kinetic Theory and Hydrodynamics for Poiseuille Flow, *J. Stat. Phys.*, **109** (2002), 495.
[31] K. Xu and Z.H. Li, Microchannel flows in slip flow regime: BGK-Burnett solutions, *J. Fluid Mech.*, **513** (2004), 87.
[32] K. Xu, Super-Burnett solutions for Poiseuille flow, *Phys. Fluids*, **15**:7 (2003), 2077-2080.
[33] F.J. Alexander, A.L. Garcia, and B.J. Alder, Direct simulation Monte Carlo for thin-film bearings, *Phys. Fluids*, **6**:12 (1994), 3854-3860.
[34] K. Xu and E. Josyula, A multiple translational temperature model and its shock structure solution, *Phys. Rev. E*, **71** (2005), 056308.